

# PROCEEDINGS REPRINT

 SPIE—The International Society for Optical Engineering

*Reprinted from*

## ***Optical Materials Reliability and Testing: Benign and Adverse Environments***

8–9 September 1992  
Boston, Massachusetts



**Volume 1791**

## The influence of solubility on the reliability of optical fiber

M. John Matthewson  
Vincenzo V. Rondinella

Rutgers University, Fiber Optic Materials Research Program  
Department of Ceramic Science and Engineering  
Piscataway, New Jersey 08855

Charles R. Kurkjian

AT&T Bell Laboratories  
600 Mountain Avenue  
Murray Hill, New Jersey 07974

### ABSTRACT

Recent advances in the understanding of reliability of silica optical fiber indicate that the chemical durability of the fiber can control the long duration lifetime both under stress-induced fatigue and zero-stress aging conditions. In particular, dissolution of surface material produces strength degrading surface roughness. These mechanisms are discussed and strategies for improving reliability by inhibiting dissolution are examined. As an example, a modified polymer coating formulation is described that is shown to increase the lifetime of the fiber by up to a factor of thirty-fold. Strategies for improving the strength and durability of non-oxide fibers using a similar approach are also discussed.

### 1. INTRODUCTION

The fatigue, or delayed failure, exhibited by oxide glasses containing micro-cracks is now well understood, at least qualitatively. The phenomenon is attributed to the combined action of stress and an environmental reactant which is usually water. The water reacts preferentially with bonds at the tip of a defect or crack due to the concentration of stress at that position; the stress acts to reduce the activation energy of the chemical reaction. One such reaction proposed by Michalske and Freiman<sup>1</sup> is shown schematically in Fig. 1 for the attack of a siloxane bond in silica by water. The rupture of the bond causes the local crack front to advance by one bond spacing; the force supported by the broken bond is transferred to an adjacent bond and the process proceeds until the stress at the crack tip exceeds the strength of the material and catastrophic failure occurs.

It has been found empirically<sup>2</sup> that the rate of bond rupture is dependent on the intensity of the local stress field around the crack tip, as quantified by the stress intensity factor,  $K_I$ . A simple chemical rate theory predicts that the crack velocity,  $\dot{c}$ , is given by:<sup>3,4</sup>

$$\dot{c} = A' \exp \left[ n' \left( \frac{K_I}{K_{IC}} \right) \right] \quad (1)$$

where  $A'$  and  $n'$  are material parameters and  $K_{IC}$  is the material's toughness. This equation may be integrated under conditions of constant applied stress,  $\sigma_a$ , to give the time to failure,  $t_f$ .<sup>5</sup>

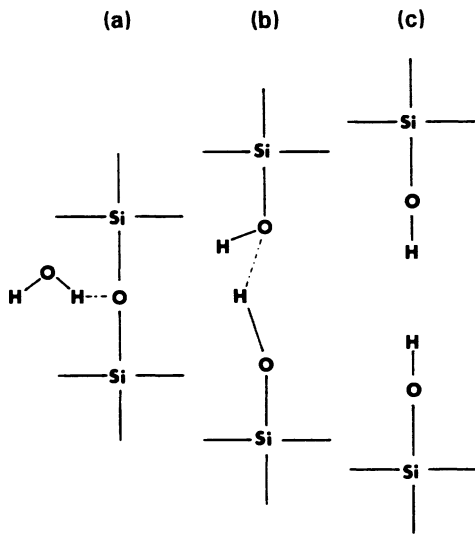


Fig. 1. Steps in the hydrolysis of a siloxane bond (after ref. 1).

$$t_f = \frac{2K_{IC}^2}{A'Y^2n'\sigma_a^2} \left( \frac{\sigma}{\sigma_i} + \frac{1}{n'} \right) \exp \left[ -n' \left( \frac{\sigma}{\sigma_i} \right) \right] \quad (2)$$

where  $Y$  is a parameter of order unity describing the crack geometry, and  $\sigma_i$  is the intrinsic strength of the glass (*i.e.* the strength in the absence of fatigue). Eq. 2 is the basis for lifetime predictions if the fatigue parameters,  $A'$  and  $n'$ , are determined by fitting to the results of accelerated tests. If  $\sigma_a$  is interpreted as the in-service stress then  $t_f$  gives the expected lifetime. Alternatively, if  $t_f$  is the design life,  $\sigma_a$  can be interpreted as the maximum allowed service stress.

In practice a power law form of Eq. 1 is almost always employed because of its mathematical simplicity. However, there are good arguments against using this form of the crack growth kinetics equation; firstly, it is not based on any physical model and secondly because, under all circumstances, the power law predicts longer lifetimes than other kinetic models frequently used and therefore lacks design conservatism.<sup>6,7</sup>

There is some question of the applicability of this model for fatigue to silica optical fiber. Kurkjian and Paek<sup>8</sup> showed that the strength of pristine fiber (greater than a few GPa) is essentially single valued, and under inert conditions is close to the theoretical strength of the material. They therefore concluded that pristine fiber is essentially flaw free. Such fibers do fail by fracture and thus the failure process includes nucleation as well as propagation of the crack. The nucleation kinetics are not included in the subcritical crack growth model outlined above. Relatively weak fiber (50-1000 MPa) is usually weak due to extrinsic defects such as abrasion damage or adhering particles. Such fiber is also not expected to have well defined sharp cracks, and any cracks that might be present are expected to be subjected to residual stresses left by the process that introduced the defect.<sup>9,10</sup>

Despite these difficulties, the subcritical crack growth model can be used as a semi-empirical model for extrapolating accelerated fatigue data. Fig. 2, for example, shows static fatigue data obtained for polymer coated fiber tested in 22°C pH 7 buffer solution. Also shown are extrapolations of these data (using the techniques of Matthewson<sup>7</sup>) out to a typical service life of 25 years. The solid lines are the best fit predictions of both the power law and exponential (Eq. 1) kinetics models; the dashed lines represent 95% confidence intervals on the predictions and arise from the statistical scatter in the data. While different kinetics models give different results, the statistical uncertainty is reasonably small. Therefore, if an appropriately conservative crack growth kinetics model is used, reasonable reliability predictions can be made. However, this process is a *semi-empirical*

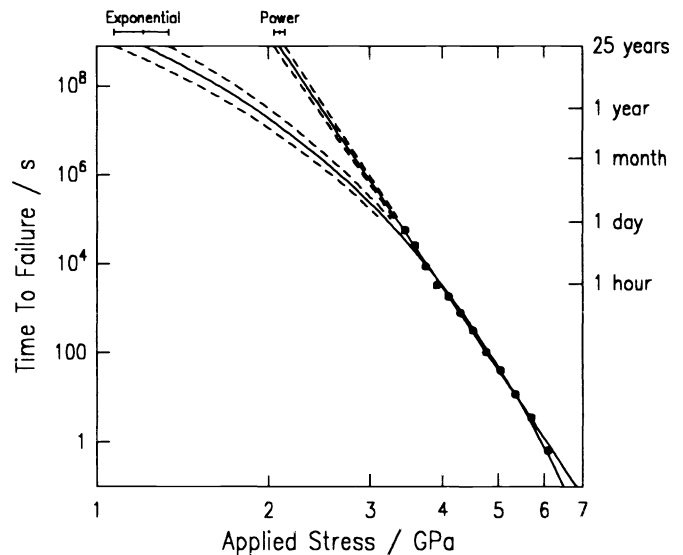


Fig. 2. Extrapolation of accelerated data to a 25 year lifetime for the power law and exponential (Eq. 1) crack growth kinetics models. Measurements were made on coated fiber in 22°C pH 7 buffer.

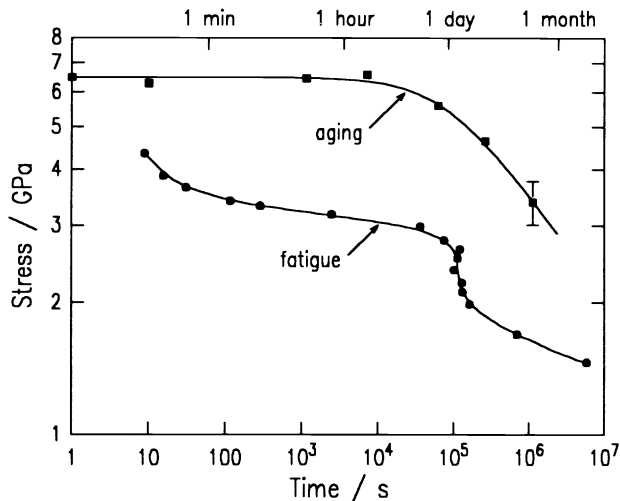


Fig. 3. Static fatigue (●) (applied stress vs. time to failure) and zero stress aging (■) (residual strength vs. aging time) for epoxy-acrylate coated fiber in 100°C water (data from ref. 11).

The position and nature of the knee are not dependent on the presence of a polymer coating since it has been observed for bare fiber.<sup>12,11</sup> However, it is thought to be sensitive to coating properties such as adhesion.<sup>13,14</sup> The knee has only been observed for fibers tested in liquid aqueous environments, except for the first data that exhibited the phenomenon which were obtained in humid air.<sup>15</sup> Recent advances have clarified the mechanisms leading to the knee.

Kurkjian, Krause and Paek<sup>16</sup> pointed out that high strength fiber aged in hot water degrades in strength down to approximately 2.5 GPa and that initially weak silica rods are strengthened by aging also to ~2.5 GPa. They proposed that this similarity in strength resulted from surface roughness of similar shape but different scale for the two cases; *i.e.* that ellipsoidal etch pits form in the surface of the fiber. Matthewson and Kurkjian<sup>11</sup> showed that the onset in the strength degradation under zero stress aging conditions occurred at a similar time to the onset of the fatigue knee. Both sets of data are superimposed in Fig. 3. This result indicates that the fatigue knee is closely related to the zero stress aging behavior and results from the same mechanism.

During the course of their experiments Matthewson and Kurkjian (unpublished data) observed that in 1M KOH (pH 14), for a given applied stress in the post-knee region, a narrow distribution of failure times was produced, but that the mean time to failure could vary by up to a factor of 10. This variability was eventually found to depend on how long the KOH had been in the apparatus before use. Fig. 4 shows their results which indicate that the older KOH gives longer times to failure and is therefore less aggressive. Their explanation for this phenomenon was that the KOH slowly dissolves silica and boria from the borosilicate glassware used in the apparatus and that increasing

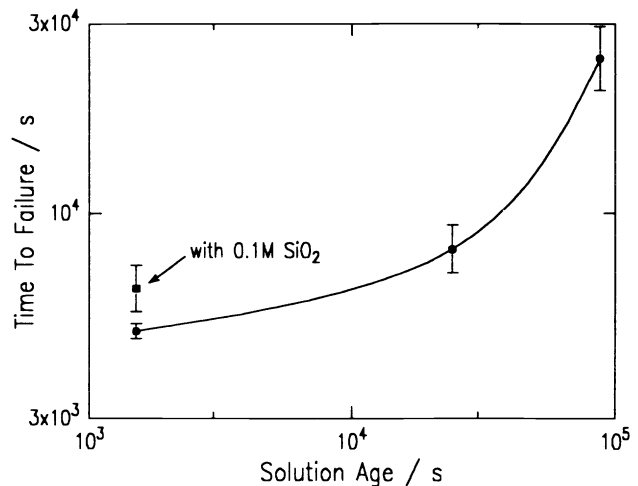


Fig. 4. Time to failure vs. solution age for static fatigue of fiber in 90°C 1M KOH at 1.2 GPa.

extrapolation since the details of the fatigue process in high strength silica are not clearly understood. Therefore, such predictions are only valid if there is no change of behavior or change of mechanism beyond the range of accelerated tests. Unfortunately, it is now well established that under some conditions there is indeed a change of behavior at long times to failure, low applied stress - the fatigue "knee" or "transition" - beyond which fatigue progresses at an accelerated rate. However, if the onset of the knee can be sufficiently delayed in time, the subcritical crack growth model could still be used to make reliability predictions. The purpose of this paper is to discuss the mechanism that leads to the fatigue knee and to present one strategy for delaying it.

## 2. THE FATIGUE "KNEE"

Fig. 3 shows static fatigue data for UV-curable epoxy-acrylate coated silica fiber in 100°C water which<sup>11</sup> exhibit the typical fatigue in which there is an abrupt change in slope for times to failure above 10<sup>5</sup>s.

quantities of silica (or perhaps boria) in solution slows the etch pit formation proposed by Kurkjian, Krause and Paek.<sup>16</sup> They found that adding sodium silicate to the KOH to give 0.1M SiO<sub>2</sub> in solution increased the time to failure (Fig. 4). The increase is only modest since the sodium silicate increases the pH of the KOH which tends to counteract the effect of the dissolved silica. It was these results the lead to the ideas outlined in this paper.

Yuce and coworkers verified the formation of surface roughness during aging by imaging the fiber surface using scanning tunneling microscopy<sup>17</sup> and atomic force microscopy (AFM).<sup>18</sup> They found that the magnitude of the roughness correlated with residual strength after aging. Interestingly, they found that while the degradation kinetics varied with the coating material for a range of coatings, the different coatings yielded unique roughness/strength behavior.<sup>18</sup>

The above observations indicate that the fatigue knee is caused by surface etching. The etch pits then behave as stress concentrations which lead to nucleation of a crack and subsequent failure. This implies that the pre-knee behavior is characterized by propagation of existing "defects" while the post-knee behavior is characterized by formation of surface roughness which then acts as the defect.

## 2.1 The Role of Dissolution

The formation of surface etch pits, discussed above, clearly requires removal of silica from the glass surface. This process of dissolution is quite distinct from the mechanism of crack growth discussed in the introduction, which only requires bond rupture along a plane. The etching process differs in two key ways; firstly it involves material removal, in the form of silicic acid, Si(OH)<sub>4</sub>, and secondly it is a surface reaction free of the steric hindrance at the tip of a sharp crack.

This mechanism for the fatigue knee implies that the fiber reliability can be improved if the dissolution chemical reaction can be slowed. Perhaps the most obvious way to achieve this is to introduce the product of the reaction into the environment, as exemplified in Fig. 4. This has been achieved by introducing colloidal silica into the polymer coating of the fiber. These small particles are more soluble than the fiber due to their curvature and so, it is thought, preferentially dissolve as the environmental water penetrates the coating. The partially saturated water then has a reduced activity at the glass surface.

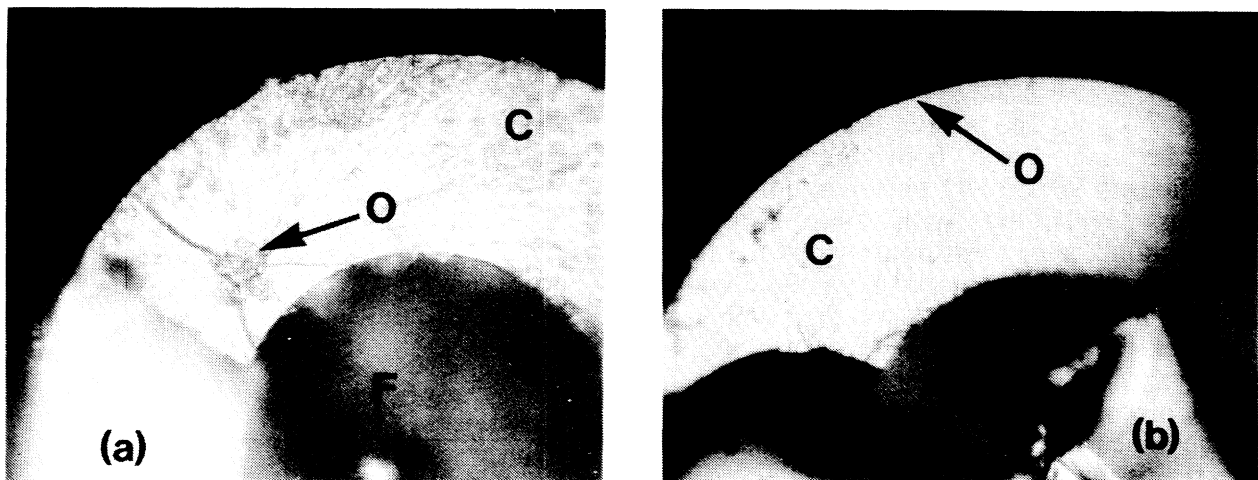


Fig. 5. Fracture surface of the epoxy-acrylate coating (C) showing the glass fiber (F) and the fracture origin (O) for (a) "with" and (b) "without" fiber.

### 3. RESULTS

Two lengths of 125  $\mu\text{m}$  diameter silica fiber were drawn; each with a UV-curable epoxy- acrylate coating with an outside diameter of 250  $\mu\text{m}$ . One coating (denoted "with") contained 0.7 wt% of grade M5 Cab-O-Sil silica particles with  $\sim 30$  nm diameter and a surface area of  $\sim 200$   $\text{m}^2\cdot\text{g}^{-1}$ .<sup>19</sup> The other coating (denoted "without") did not have any silica added and acted as a control.

The silica particles were introduced into the "with" coating by manually stirring into the pre-polymer. This procedure did not fully disperse the particles since the coating appeared milky and agglomerates were visible in the optical microscope. These agglomerates sometimes acted as origins for fracture of the coating when breaking the fiber (Fig.

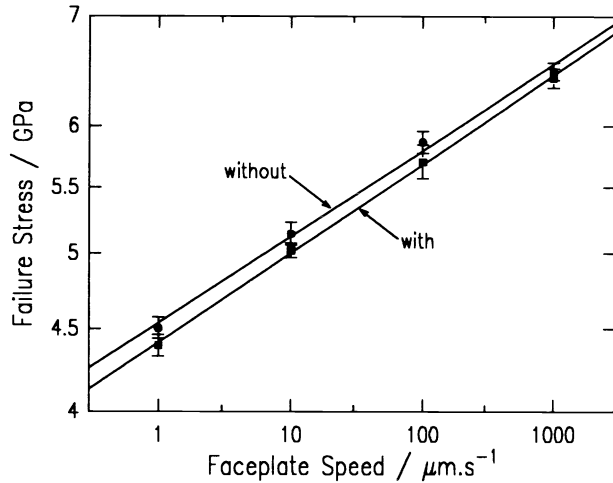


Fig. 6. Dynamic fatigue of "with" (■) and "without" (●) fiber in two-point bending.

5a), while the "without" coating typically fractured from its inner or outer surface (Fig. 5b). However, the position of the coating fracture origin is unlikely to affect the fiber strength.

#### 3.1 Strength

Fig. 6 shows the results of short term dynamic fatigue experiments performed in 2-point bending<sup>20,21</sup> on the "with" and "without" fiber. The strengths and slopes are similar implying that the "with" fiber strength has not been degraded by the presence of agglomerates in the coating, and that the fatigue behavior of both fibers is essentially identical.

The tensile strengths of 150 mm lengths of fiber were measured in 20%rh, 22°C air at a loading rate of 500  $\text{MPa}\cdot\text{s}^{-1}$ . The "without" fiber had a strength of  $5.55 \pm 0.03$  GPa while the "with" fiber was somewhat weaker at  $3.22 \pm 0.22$  GPa with a significantly broader spread of values. It is therefore likely that the agglomerates in the "with" coating can occasionally damage the fiber, probably at the capstan grips. However, this problem could be avoided by better dispersion of the silica in the coating.

#### 3.2 Static Fatigue

Fig. 7 shows the results of static fatigue in two-point bending<sup>22</sup> for both the "with" and "without" fiber in 90°C pH 7 buffer solution. At all applied stress levels, the "with" fiber lasts longer than the "without" and, most significantly the fatigue knee, which occurs at about  $10^4$  s for the "without" fiber, is delayed until  $\sim 5 \times 10^6$  s for the "with" fiber with an overall improvement of a factor of 30 or more. At applied stresses less than 2.5 GPa, the lifetime is prolonged by at least a factor of 3 by having the silica in the coating. At the lowest applied stresses the behavior of the two fibers appear to converge. This might be because the protection mechanism becomes exhausted after a sufficiently

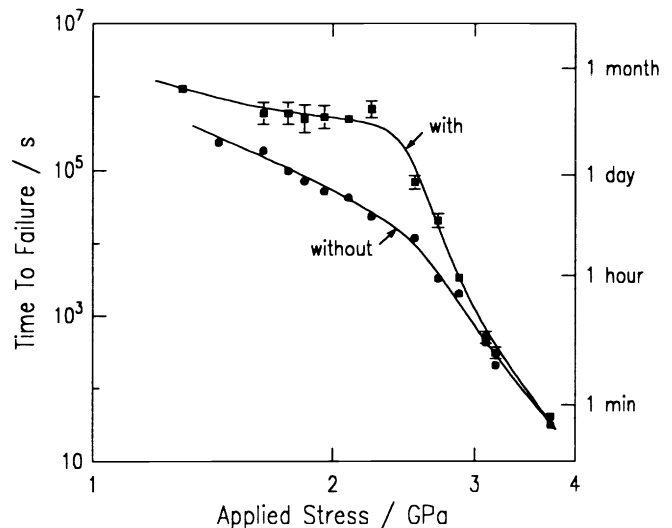


Fig. 7. Static fatigue behavior of "with" (■) and "without" (●) fiber in 90°C pH 7 buffer.

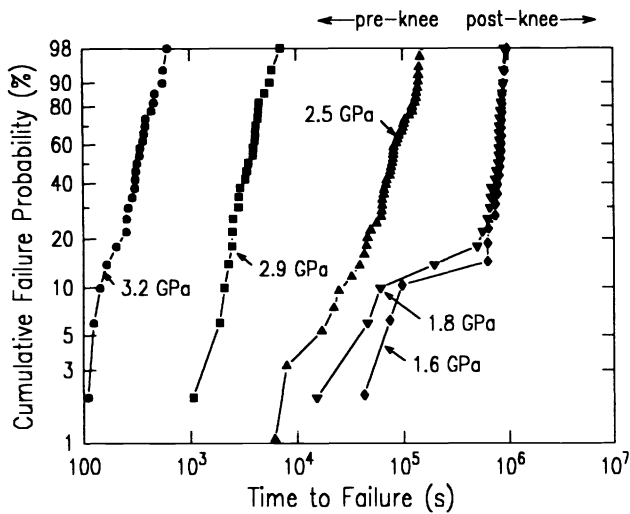


Fig. 8. Weibull probability plots of some of the data of Fig. 7.

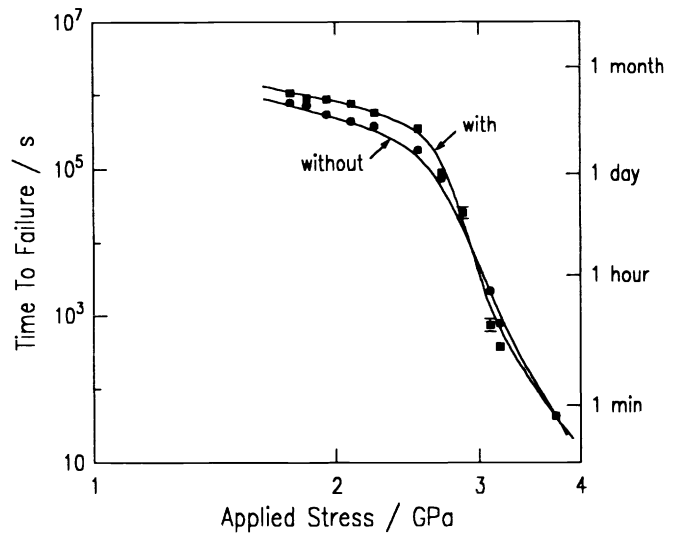


Fig. 9. Static fatigue behavior of "with" (■) and "without" (●) fibers in 90°C pH 4 buffer.

long duration. Increasing the small amount of silica in the coating used in these experiments may well prolong the efficacy of the coating.

The error bars for the "with" fiber data in Fig. 7 are generally larger than those for the "without" fiber. Fig. 8 shows Weibull plots of representative points from the "with" data of Fig. 7. In the post-knee region (applied stress < 2.4 GPa) the lines are steeper (higher Weibull modulus) than in the pre-knee region, as is expected since the local value of the fatigue parameter,  $n$ , is lower past the knee.<sup>23,11</sup> However, a low strength mode is observed in the knee region. The failure times of the low strength mode are similar to those of the "without" fiber. The low strength mode is therefore probably due to regions of the coating having little or no silica particles due to the poor dispersion. Better dispersion should lead to removal of the low strength mode and further improvement.

Fig. 9 shows static fatigue results for both coatings in pH 4 buffer solution. Again, the "with" fiber has improved behavior with double the lifetime in the post-knee region, though not as pronounced as in the pH 7 environment. Results in pH 10 buffer reported elsewhere<sup>24</sup> show similar benefits though, again, not as great as in pH 7. Therefore, this scheme for improving fiber reliability is effective across a broad range of pH but is most effective under neutral conditions.

### 3.3 Zero Stress Aging Behavior

Fig. 10 shows the post-aging strength of "with" and "without" fiber, measured at room temperature in pH 7 buffer solution, as a function of aging time in 90°C pH 7 buffer. There is an initial rapid decrease in strength over the first few hours, and then a more gradual one. Under all conditions the "with" fiber has a significantly higher residual strength than the "without" fiber.

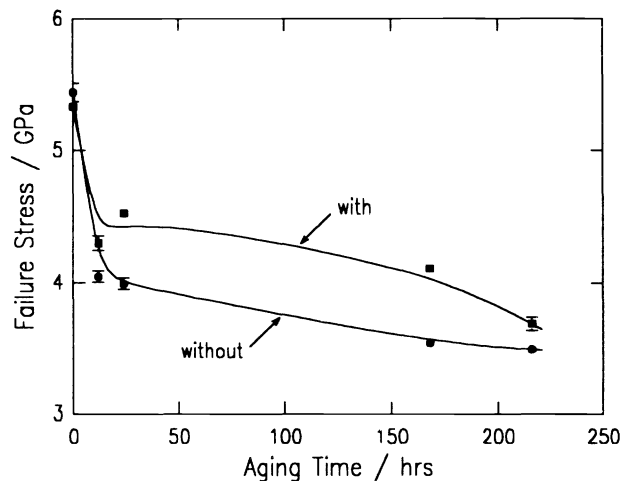


Fig. 10. Post aging residual strength behavior of "with" (■) and "without" (●) fiber aged in 90°C pH 7 buffer.

### 3.4 AFM Profilometry

Specimens of aged fiber have been stripped using 200°C concentrated sulfuric acid and atomic force microscopy (AFM) has been used to examine the fiber surface profile. Fig. 11 shows AFM images of (a) unaged fiber and (b) "without" and (c) "with" fiber aged for 168 hours in 90°C pH 7 buffer solution.

The "without" fiber is substantially roughened by aging (1.36 nm rms roughness compared with 0.30 nm for the unaged fiber). In contrast, the "with" fiber has a surface roughness of only 0.46 nm. These results clearly show the efficacy of the coating additive in suppressing the development of the surface roughness and consequent strength loss.

Examination of Fig. 11 shows that the frequency as well as amplitude of surface roughness is modified by aging, with the unaged specimen having much longer wavelength undulations. Fig. 12 shows the spectral distribution of the surface roughness. These spectra must be interpreted carefully since the AFM control software† normalizes the spectra to the peak wavelength so each spectrum has a different vertical scale. The peaks near DC (infinite wavelength) represent overall curvature of the fiber surface and so can be ignored. (Note that the AFM control software can only remove curvature in the  $x$  and  $y$  directions consecutively; this leaves residual curvature at 45° to these axes. Simultaneous removal of  $x$  and  $y$  curvature is required to remove the overall curvature of the fiber surface). The unaged fiber tends to only have long wavelength components and has relatively small spectral content for wavelengths less than 150 nm or so. In contrast, the "without" fiber has significant spectral content down to ~45 nm while the "with" fiber has a broad spectrum extending down to ~20 nm. The longer wavelengths of the unaged fiber are a function of conditions during the fiber drawing process and depend on, amongst other things, the distribution of viscosity fluctuations at the draw temperature. In contrast, the surface profile of the aged specimens depends on the fluctuation of chemical activity in the amorphous surface and is of much shorter wavelength. The spectral content is important since the stress magnification of an etch pit depends both on its depth and tip curvature, and in this way on its width. Higher frequency components in the roughness spectrum mean narrower, sharper pits with greater associated strength degradation.

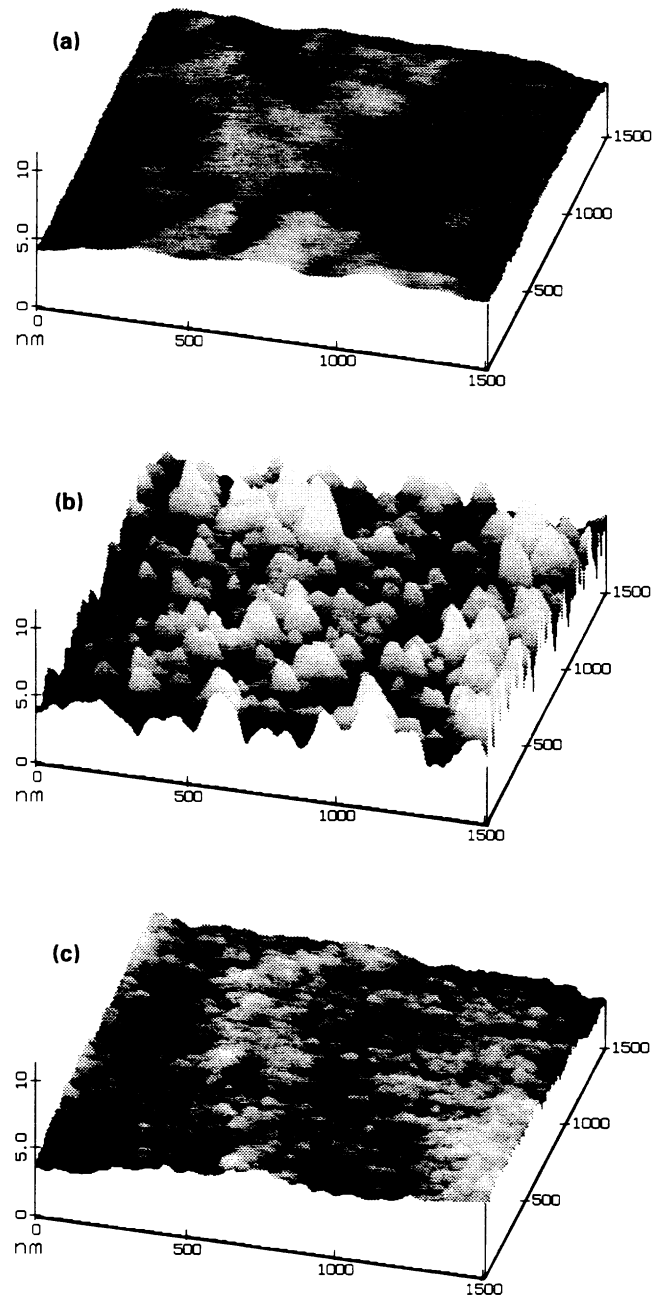


Fig. 11. AFM profiles of the surface of (a) unaged and (b) "without" and (c) "with" fiber aged for 168 hours in 90°C pH 7 buffer.

† Nanoscope II, software version 5.4, Digital Instruments, Santa Barbara, CA.

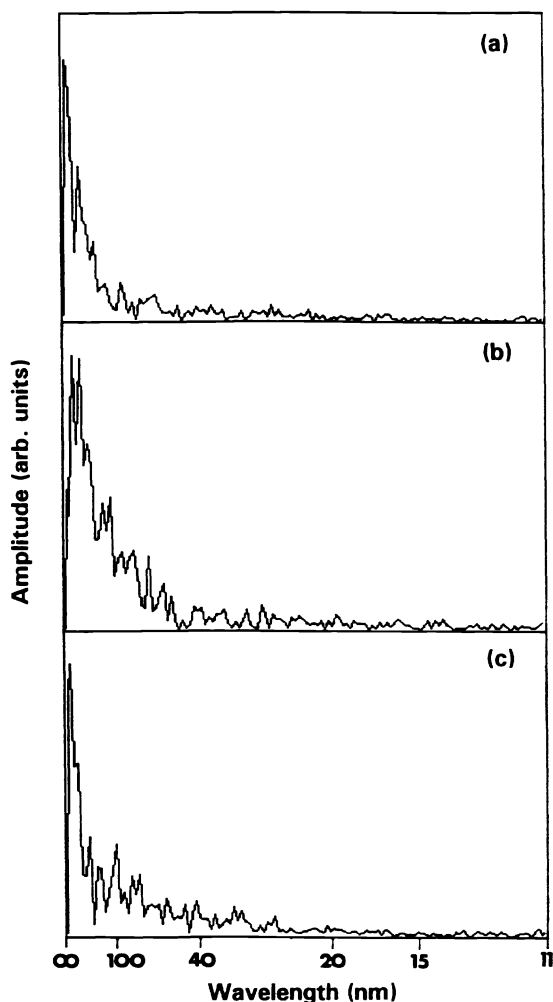


Fig. 12. Surface roughness spectra for the profiles of Fig. 12, (a) unaged and (b) "without" and (c) "with" fiber aged for 168 hours in 90°C pH 7 buffer.

and polyimides. Also the technique is applicable to other glass systems. Multi-component glass systems could also be protected by adding appropriate components of the glass to the coating; presumably the more soluble components. This would be very useful for the heavy metal fluoride glasses whose mechanical properties are dominated by their poor durability in water.

This technique should prove in practice to be a relatively inexpensive approach to improving fiber reliability. The particles can be added to existing prepolymer coating formulations. A mixing and degassing step is added to the manufacturing process and it might be necessary to heat the prepolymer in order to offset the increase in viscosity the particles cause. However, in critical applications, this added expense must be weighed against the substantial improvements in mechanical reliability.

## 5. ACKNOWLEDGEMENTS

We are indebted to F. V. DiMarcello and R. G. Huff (AT&T Bell Laboratories) for drawing the fiber used in this study, and to W. M. Russ, E. S. Chang and J. R. Hamblin for help in obtaining data.

## 4. DISCUSSION AND CONCLUSIONS

This paper presents results for the mechanical behavior of an optical fiber whose polymer coating has been loaded with a small quantity (0.7 wt%) of colloidal silica. This prototype fiber could be improved in many ways. In particular, the poor dispersion of the silica particles in the coating leads to occasional weak specimens measured in tension, presumably due to surface damage by hard agglomerates of particles, and to increased scatter in static fatigue results. However, despite these imperfections, the coating additive results in substantial improvements in both the static fatigue and zero stress aging behavior. In particular, the fatigue knee onset is delayed in time by almost two decades at pH 7. This delay is significant since, with our current level of understanding, the presence, or absence, and position of the fatigue knee cannot be predicted *a priori*. The presence of the knee invalidates any reliability predictions made by extrapolating short term data using the subcritical crack growth model. If the knee can be delayed so that it does not occur during the design life of a fiber in more moderate environments, then the reliability predictions can be made with more confidence.

Further improvements over the already substantial performance benefits of the particle additive can be made by better dispersing the particles in the coating. Also, adding more particles should bring further improvements, as will optimizing the particle sizes.

This technique of adding suitable particles to the coating in order to suppress etching of the fiber surface by environmental moisture can readily be extended to other systems. The particles are easily added to other coating materials while in their liquid state, such as the silicones

## 6. REFERENCES

1. T. A. Michalske and S. W. Freiman, "A Molecular Mechanism for Stress Corrosion in Vitreous Silica," *J. Am. Ceram. Soc.*, **66** [4] 284-288 (1983).
2. A. G. Evans, S. M. Wiederhorn, "Proof testing of ceramic materials - an analytical basis for failure prediction," *Int. J. Fracture* **10** [3] 379-92 (1974).
3. W. B. Hillig and R. J. Charles, "Surfaces, Stress-Dependent Surface Reactions, and Strength," in "High Strength Materials," ed. V. F. Zackay, Wiley, New York, pp 682-705 (1965).
4. S. M. Wiederhorn and L. H. Bolz, "Stress Corrosion and Static Fatigue of Glass," *J. Am. Ceram. Soc.*, **53** [10] 543-549 (1970).
5. K. Jakus, J. E. Ritter, Jr, and J. M. Sullivan, "Dependency of Fatigue Predictions on the Form of the Crack Velocity Equation," *J. Am. Ceram. Soc.*, **64** [6] 372-374 (1981).
6. G. M. Bubel and M. J. Matthewson, "Optical Fiber Reliability Implications of Uncertainty in the Fatigue Crack Growth Model," *Opt. Eng.* **30** [6] 737-745 (1991).
7. M. J. Matthewson, "Fiber Lifetime Predictions," *Proc. SPIE, Symp. on Fiber Optic Components and Reliability*, **1580** 130-41 (1991).
8. C. R. Kurkjian and U. C. Paek, "Single-Valued Strength of "Perfect" Silica Fibers," *Appl. Phys. Lett.*, **42** [3] 251-253 (1983).
9. T. P. Dabbs, B. R. Lawn, "Strength and fatigue properties of optical glass fibers containing microindentation flaws," *J. Am. Ceram. Soc.*, **68** [11] 563-569 (1985).
10. B. Lin, M. J. Matthewson & G. J. Nelson, "Indentation Experiments in Silica Optical Fibers," *Proc. SPIE "Fiber Optic Reliability: Benign and Adverse Environments IV,"* **1366** 157-166 (1990)
11. M. J. Matthewson and C. R. Kurkjian, "Environmental Effects on the Static Fatigue of Silica Optical Fiber," *J. Am. Ceram. Soc.* **71** [3] 177-183 (1988).
12. J. T. Krause, "Zero Stress Strength Reduction and Transitions in Static Fatigue of Fused Silica Fiber Lightguides," *J. Non-Cryst. Solids*, **38 & 39** 497-502 (1980).
13. J. P. Clarkin, B. J. Skutnik and B. D. Munsey, "Enhanced Strength and Fatigue Resistance of Silica Fibers with Hard Polymeric Coatings," *J. Non-Cryst. Solids*, **102** 106-111 (1988).
14. T. S. Wei and B. J. Skutnik, "Effect of Coating on Fatigue Behavior of Optical Fiber," *J. Non-Cryst. Solids*, **102** 100-105 (1988).
15. T. T. Wang and H. M. Zupko, "Long-Term Mechanical Behaviour of Optical Fibres Coated with a UV-Curable Epoxy Acrylate," *J. Mat. Sci.*, **13** 2241-2248 (1978).
16. C. R. Kurkjian, J. T. Krause and U. C. Paek, "Tensile Strength Characteristics of "Perfect" Silica Fibers," *J. de Phys.*, **43** [12] C9-585-586 (1982).
17. R. S. Robinson and H. H. Yuce, "Scanning Tunneling Microscopy Study of Optical Fiber Corrosion: Surface Roughness Contribution to Zero-Stress Aging," *J. Am. Ceram. Soc.*, **74** [4] 814-18 (1991).
18. H. H. Yuce, J. P. Varachi Jr., J. P. Kilmer, C. R. Kurkjian and M. J. Matthewson, "Optical Fiber Corrosion: Coating Contribution to Zero-Stress Aging," *OFC'92 Tech. Digest*, post deadline paper PD21, San Diego, CA, 1992.
19. "Cab-O-Sil Properties and Functions," Cabot Corp., Tuscola, IL (1983).
20. P. W. France, M. J. Paradine, M. H. Reeve and G. R. Newns, "Liquid Nitrogen Strengths of Coated Optical Glass Fibres," *J. Mat. Sci.* **15** 825-30 (1980).
21. M. J. Matthewson, C. R. Kurkjian and S. T. Gulati, "Strength Measurement of Optical Fibers by Bending," *J. Am. Ceram. Soc.*, **69** [11] 815-821 (1986).
22. M. J. Matthewson and C. R. Kurkjian, "Static Fatigue of Optical Fibers in Bending," *J. Am. Ceram. Soc.*, **70** [9] 662-668 (1987).
23. P. L. Key, A. Fox and E. O. Fuchs, "Mechanical Reliability of Optical Fibers," *J. Non-Cryst. Solids* **38 & 39** 463-468 (1980).
24. V. V. Rondinella, M. J. Matthewson and C. R. Kurkjian, "Coating Additives for Improved Mechanical Reliability of Optical Fiber," submitted *J. Am. Ceram. Soc.*, 1992.